NANOSCOPIC MOLECULAR CLUSTER V$_{15}$: HIGH-FIELD EPR AND MAGNETIZATION AT ULTRA-LOW TEMPERATURES[§]

Boris Tsukerblat,[a] Alex Tarantul,[a] Achim Müller [b]

[a] *Department of Chemistry, Ben-Gurion University of the Negev, 84105 Beer-Sheva, Israel, e-mail: tsuker@bgumail.bgu.ac.il*
[b] *Fakultät für Chemie, Universität Bielefeld - 33501 Bielefeld, Germany, e-mail: a.mueller@uni-bielefeld.de*

*In memory of Professor Yurii E. Perlin on the occasion of his 90 th birthday –
to highlight his exceptional achievements and kudos*

Abstract: In this paper we give a short overview of our efforts in the understanding of the magnetic properties of the fascinating nanoscopic cluster $K_6[V^{IV}_{15}As_6O_{42}(H_2O)]\cdot 8H_2O$ (hereafter V$_{15}$) exhibiting layers of magnetization. We analyze EPR and adiabatic magnetization of the V$_{15}$ cluster with a triangular V^{IV}_3 array causing spin frustration. A model for V$_{15}$ includes isotropic and antisymmetric (AS) exchange interactions in the general form compatible with the trigonal symmetry. Orientation of the AS vector (but not only its absolute value) is shown to play an important physical role in spin-frustrated systems. We were able to reach perfect fit to the experimental data on the stepwise dependence of magnetization vs. field at ultra-low temperatures. Furthermore, it was possible for the first time to estimate precisely two components of the AS vector coupling constant, namely, in-plane component and the perpendicular part. We show that only intramultiplet transitions in EPR are allowed when the vector of AS exchange is normal to the plane of vanadium triangle, meanwhile the in-plane part of AS exchange gives rise to a series of weak intermultiplet transitions. Experimental data on high-frequency EPR of V$_{15}$ at low temperatures are discussed. The spin-vibronic effects in trimeric spin frustrated clusters are also studied and an important role of the interplay between the AS exchange and Jahn-Teller interaction is revealed. The results clarify the concept of spin-frustration in view of its magnetic and spectroscopic manifestations in metal clusters.

Keywords: nanoscopic molecular magnets; V$_{15}$ cluster; antisymmetric exchange; Jahn-Teller effect.

1. INTRODUCTION

During the past decade growing attention has been attracted by a large unique cluster anion present in $K_6[V^{IV}_{15}As_6O_{42}(H_2O)]\cdot 8H_2O$ containing 15 ions V^{IV} (S_i=1/2) and exhibiting layers of different magnetizations [1–4]. The discovery of this fascinating system [1] opened a new trend in molecular magnetism closely related to the promising field of single molecule magnets that is expected to give a revolutionary impact on the design of new memory storage devices of molecular size and quantum computing. Studies of the adiabatic magnetization and quantum dynamics show that the V$_{15}$ cluster exhibits the hysteresis loop of magnetization [5–10] of molecular origin and can be referred to as a mesoscopic system on the border line between classical and quantum word. The studies of the static magnetic susceptibility [3,4], energy pattern [11–18] and inelastic neutron scattering [19,20] showed that the low lying part of the energy spectrum is well isolated from the remaining spin levels and can be understood as a result of interaction between three moieties consisting of five strongly coupled spins giving rise to spin S_i=1/2 of each moiety. The three-spin model for the low lying excitations so far suggested [3,7] includes isotropic Heisenberg-Dirac-Van Vleck (HDVV) exchange interaction and AS exchange firstly proposed by Dzyaloshinsky [21] and Moria [22] as an origin of spin canting. The understanding of the role of the AS exchange in spin frustrated systems dates back to the seventies (see review article [23] and references therein). AS exchange was shown to result in a zero-field splitting of the frustrated ground state of the half-integer triangular spin systems, magnetic anisotropy, essential peculiarities of the EPR spectra and wide range of phenomena related to hyperfine interactions [23–35]. Some of the conclusions of these early papers have been mentioned later [17], in particular, those regarding the zero-field splitting and Kramers theorem (see [36]).

Hereunder we give a short overview of the magnetic interactions in V$_{15}$ system with the emphasis on the manifestations of AS exchange. The three spin model is analyzed and applied to the study of energy level crossover in magnetic fields of different directions and such phenomena as low-temperature EPR, high field magnetization and structural instabilities arising from the spin-vibronic interaction and Jahn-Teller effect.

---

2. THE HAMILTONIAN, SYMMETRY PROPERTIES

The molecular cluster V_{15} has a distinct layered quasispherical structure within which fifteen V^{IV} ions ($s_i = 1/2$) are placed in a large central triangle sandwiched by two distorted (non-planar) hexagons [1,2] possessing $\mathbf{D}_3$ symmetry (Fig.1-3). Each subunit consisting of two spin-paired dimers and a spin of the triangle can be considered as an effective spin $s = 1/2$ placed in the central layer (Fig.1-3). This can be justified by consideration of the isotropic exchange parameters within the metal network J_1, J_2, J', J'' (see Fig.2,3) that have been firstly estimated in [3,4]. The parameter of the intradimer interaction in the hexagons is shown to be the leading one while the parameters J_1, J', J'' are significantly smaller and seem to be of the same order so that each spin of the central triangle is coupled to a pair of strongly coupled spins belonging to the lower and upper hexagons as shown in Fig.3. Each pentanuclear subunit consisting of two dimers (marked in bold in Fig.3) and a spin of the triangle can be considered as an effective spin $s = 1/2$ placed in the central layer so that the low lying part of the energy pattern of the system entire can be viewed as the result of spin coupling within the triangular cluster in which a relatively weak spin coupling appears through the interactions with the hexagons in their excited states. The energy pattern within the full spin space (Fig.4) is calculated with the use of our MAGPACK software [37], A Package to Calculate the Energy Levels, Bulk Magnetic Properties, and Inelastic Neutron Scattering Spectra of High Nuclearity Spin Clusters, based on the irreducible tensor operators (ITO) technique. Using this efficient tool specially designed for the study of high nuclearity clusters, one can show [36] that the ground state with total spin $S = 1/2$ and first excited state with $S = 3/2$ (Fig.4, box) are well isolated (about $400 cm^{-1}$) from the higher states thus justifying an effective triangle approximation. Although the exchange problem is tractable in full Hilbert space of 15 spins [4,14,17,18,36] ($2^{15} = 32768$ states) a model of a spin triangle proposed and substantiated in [3,4] and developed in [36] gives accurate and descriptive
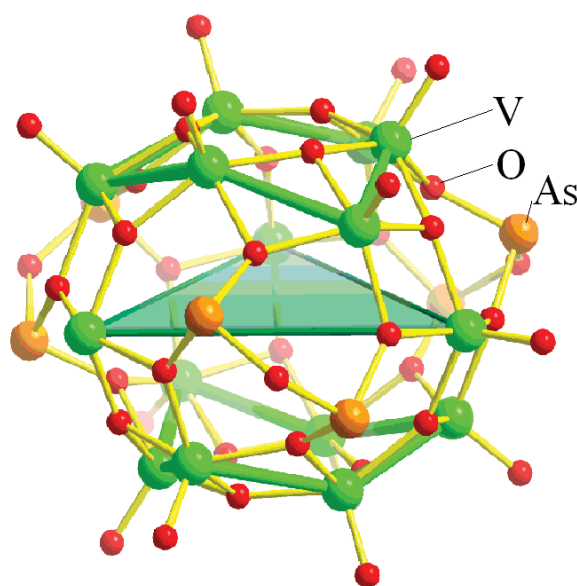
Fig. 1. The cluster anion $[V^{IV}_{15}As_6O_{42}(H_2O)]^{6-} = \{V_{15}As_6\}$: (a) ball-and-stick representation without the central water molecule emphasizing the V_3 triangle [1].

results for the low lying set of the levels and can be applied at low temperatures providing a high accuracy of calculations for all thermodynamic and spectroscopic properties below 100K. In particular, this model allows to deduce the conclusions about the role of the AS exchange [36]. The isotropic superexchange can be described by the conventional HDVV Hamiltonian that represents a solid background for the consideration of the exchange interactions in transition metal clusters. For a symmetric triangle one finds the following Hamiltonian:

$$H_0 = -2J_0 \left(S_1 S_2 + S_2 S_3 + S_3 S_1 \right),\qquad(1)$$

where $S_i = 1/2$ and J_0 is the parameter of the antiferromagnetic exchange $(J_0 < 0)$; for the sake of convenience we use a positive value $J = -J_0$ and the basis will be labeled as $|S_1 S_2 (S_{12}) S_3 SM\rangle \equiv |(S_{12}) SM\rangle$, where $S_{12} = 0, 1$. Is the intermediate spin in three-spin copling scheme. The energy pattern includes two degenerate spin

doublets and a spin quadruplet separated by the gap $3J$. The HDVV interaction is obviously magnetically isotropic that arises from is physical origin and mathematical structure of the HDVV Hamiltonian. To adequately describe EPR spectra and anisotropy of the magnetization on should take into account anisotropic magnetic interactions between the vanadium ions. First kind of such interaction is represented by the AS exchange introduced by Dzyaloshinsky [21] and Moria [22] as an origin of spin canting in non-collinear magnetic crystals. The Hamiltonian of AS exchange preserving trigonal symmetry is given by [36]:

$$H_{AS} = D_n \left([\mathbf{S}_1 \times \mathbf{S}_2]_Z + [\mathbf{S}_2 \times \mathbf{S}_3]_Z + [\mathbf{S}_3 \times \mathbf{S}_1]_Z \right)$$
$$+ D_l \left([\mathbf{S}_1 \times \mathbf{S}_2]_X - \frac{1}{2}[\mathbf{S}_2 \times \mathbf{S}_3]_X + \frac{\sqrt{3}}{2}[\mathbf{S}_2 \times \mathbf{S}_3]_Y - \frac{1}{2}[\mathbf{S}_3 \times \mathbf{S}_1]_X - \frac{\sqrt{3}}{2}[\mathbf{S}_3 \times \mathbf{S}_1]_Y \right)$$
$$+ D_t \left([\mathbf{S}_1 \times \mathbf{S}_2]_Y - \frac{\sqrt{3}}{2}[\mathbf{S}_2 \times \mathbf{S}_3]_X - \frac{1}{2}[\mathbf{S}_2 \times \mathbf{S}_3]_Y + \frac{\sqrt{3}}{2}[\mathbf{S}_3 \times \mathbf{S}_1]_X - \frac{1}{2}[\mathbf{S}_3 \times \mathbf{S}_1]_Y \right) \tag{2}$$

Here the spin operators are related to the molecular frame, the parameter D_n is associated with the normal (Z-axis) component of AS exchange, D_l and D_t are those for the in-plane parts (see details in [36]). The matrix of H_{AS} was explicitly calculated in the basis $|(S_{12})SM\rangle$ using the ITO technique [27, 38].

The analysis of the HDVV Hamiltonian (see review article [23] and references therein) revealed that the "degeneracy doubling" in the ground spin-frustrated state $(S_{12})S = (0)1/2,(0)1/2$ is related to the exact orbital degeneracy so that the ground term is the orbital doublet ^2E in the trigonal symmetry. It was concluded [23] that the AS exchange acts within the $(S_{12})S = (0)1/2,(0)1/2$ manifold like a first order spin-orbital interaction within ^2E term and gives rise to two doublets in agreement with the Kramers theorem [38].
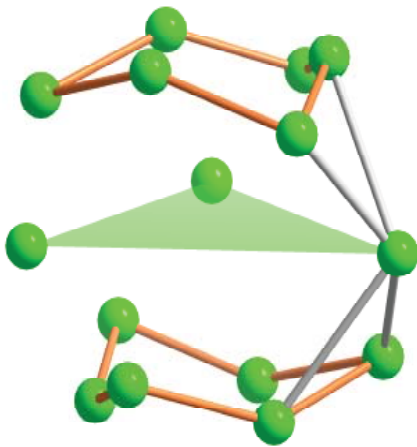
Fig. 2. Scheme of the V$_{15}$ metal network [1] in the cluster anion [V$^{IV}_{15}$As$_6$O$_{42}$(H$_2$O)]$^{6-}$ = {V$_{15}$As$_6$}.
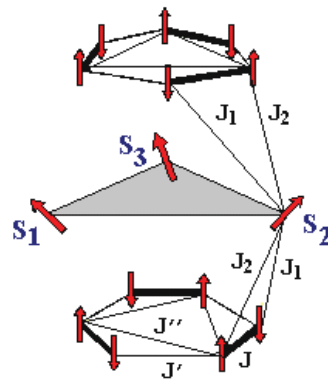
Fig. 3. Schematic structure of the metal network of V$_{15}$ cluster and pictorial representation of spin arrangement in the low lying states.

Within the pseudoangular momentum representation the basis $|(0)1/2,\pm 1/2\rangle$, $|(1)1/2,\pm 1/2\rangle$ of the irreducible representation E in trigonal point groups can be related to two projections $M_L = +1$ and $M_L = -1$ belonging to the fictitious orbital angular momentum $L=1$, the basis functions $u_{LM_L}(S,M_S) \equiv u_{M_L}(S,M_S)$ can be found as the circular superpositions [36]:

$$u_{\pm 1}(1/2, \pm 1/2) = \mp 1/\sqrt{2}\left(|(0)1/2,\pm 1/2\rangle \pm i|(1)1/2,\pm 1/2\rangle\right),$$
$$u_{\pm 1}(1/2, \mp 1/2) = \mp 1/\sqrt{2}\left(|(0)1/2,\mp 1/2\rangle \pm i|(1)1/2,\mp 1/2\rangle\right). \tag{3}$$

Using this conception one can introduce the functions $U_S(M_J)$ belonging to a definite full spin S and projections $M_J = M_L + M_S$ of the full pseudoangular momentum, so that $U_{1/2}(\pm 3/2) = u_{\pm 1}(1/2, \pm 1/2)$ and $U_{1/2}(\pm 1/2) = u_{\pm 1}(\mp 1/2)$. The quantum numbers so far introduced correspond to the Russel-Saunders coupling scheme in axial symmetry. The level with $S = 3/2$ is an orbital singlet corresponding thus to $M_L = 0$, the components are labeled as $u_0(3/2, M_S) \equiv U_{3/2}(M_J)$ with $M_S = \pm 1/2$ and $M_S = \pm 3/2$, so that $M_J = \pm 1/2$ and $\pm 3/2$.

3. THE ENERGY PATTERN IN PARALLEL FIELD

Due to the actual axial symmetry of the system reflected in the pseudoangular momentum classification of the states, the matrix of the full Hamiltonian can be blocked into four second order matrices each corresponding to a definite projection M_J of the total pseudoangular momentum. The eigen-functions of the system are found as the superpositions of states with the same M_J originating from $S = 1/2$ and $S = 3/2$ multiplets that corresponds to the *jj*-coupling scheme in axial symmetry when $S = 1/2$ and $S = 3/2$ multiplets are mixed and M_L, M_S are no longer good quantum numbers so that the eigen-states are enumerated by quantum number M_J.
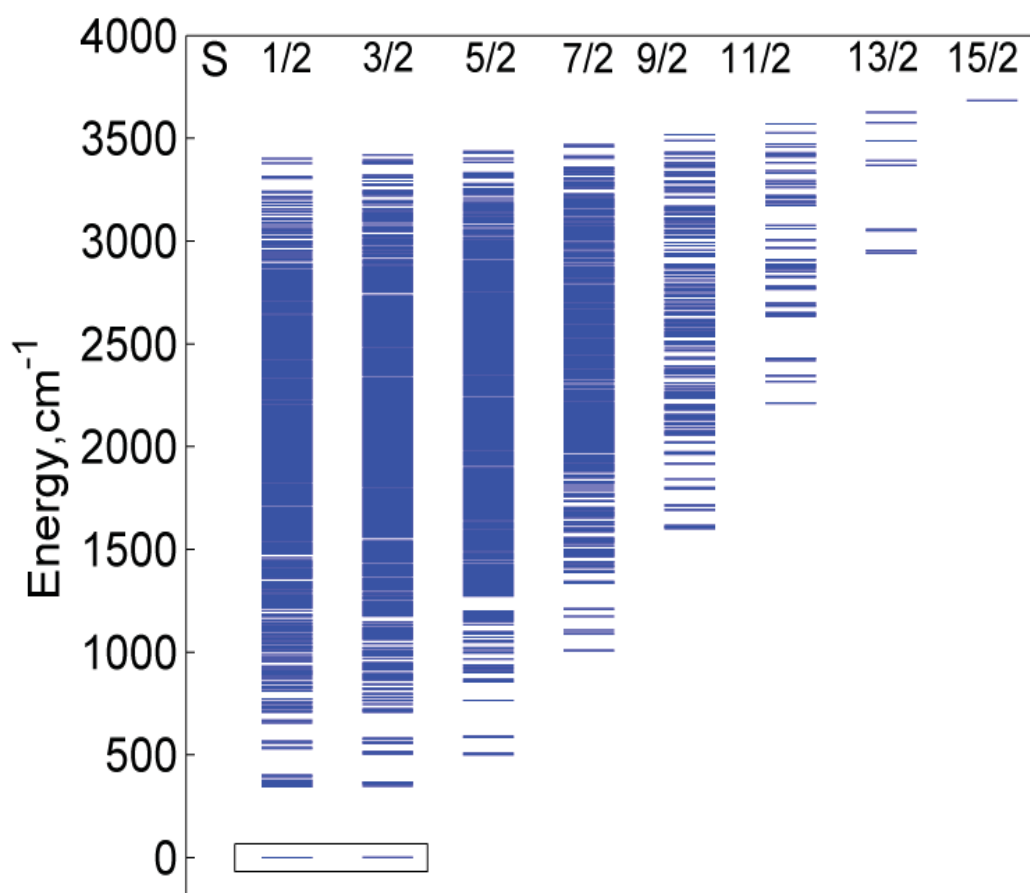
Fig. 4. Energy levels of the V_{15} cluster calculated with the parameters values from [3]. The levels are grouped accordingly to the total spin S. The calculation was performed using the MAGPACK software [37].

In absence of the field the full pattern consists of four Kramers doublets, two of them possess $M_J = \pm 1/2$ and two doublets with $M_J = \pm 3/2$. If the Zeeman interaction with the magnetic field $\mathbf{H} \parallel C_3$ axis (preserving thus axial symmetry) is also taken into account, the energy levels are enumerated by the definite values of M_J. This allows to

find the analytical solution for the energy levels providing an arbitrary interrelation between parameters (it is assumed that $g = g_{\parallel}$) [36]:

$$\varepsilon_{1,2}(H) = -\frac{1}{4}\sqrt{\left(\sqrt{3}D_n \pm 2g\beta H + 6J\right)^2 + 3D_{\perp}^2} - \frac{\sqrt{3}}{4}D_n$$

$$\varepsilon_{3,4}(H) = -\frac{1}{4}\sqrt{\left(\sqrt{3}D_n \pm 2g\beta H - 6J\right)^2 + 9D_{\perp}^2} + \frac{\sqrt{3}}{4}D_n \mp g\beta H$$

$$\varepsilon_{5,6}(H) = \frac{1}{4}\sqrt{\left(\sqrt{3}D_n \mp 2g\beta H + 6J\right)^2 + 3D_{\perp}^2} - \frac{\sqrt{3}}{4}D_n$$

$$\varepsilon_{7,8}(H) = \frac{1}{4}\sqrt{\left(\sqrt{3}D_n \pm 2g\beta H - 6J\right)^2 + 9D_{\perp}^2} + \frac{\sqrt{3}}{4}D_n \mp g\beta H \tag{4}$$

These levels are shown in Fig. 5. One can see that they do depend upon two effective parameters of AS exchange D_n and $D_{\perp}$ $\left(D_{\perp}^2 = D_t^2 + D_l^2\right)$ rather than upon three parameters D_n, D_l and D_t of the Hamiltonian. It is important that the "normal" part of the AS exchange operates only within the basis of two "accidentally" degenerate doublets $(S_{12})S = (0)1/2, (1)1/2$, meanwhile two "in-plane" contributions (terms of the Hamiltonian associated with the parameters D_l and D_t) lead only to a mixing of the ground spin doublets $(0)1/2, (1)1/2$ with the excited spin quadruplet $(1)3/2$ separated from two low lying spin doublets by the gap $3J$. AS exchange leads to the splitting of the two S=1/2 levels into two Kramers doublets with $M_J = \pm 1/2$ and $M_J = \pm 3/2$. Usually isotropic exchange is a leading interaction, so it is useful to develop the zero-field energies as series in $D_{\perp}^2/J$. The zero-field splitting of two spin doublets within this approximation $\Delta \equiv \varepsilon(M_J = \pm 3/2) - \varepsilon(M_J = \pm 1/2) \cong \sqrt{3}D_n - D_{\perp}^2/8J$ is the first order effect with respect to the normal component of AS exchange and contains also second order correction (always negative) arising from the mixing of $(S_{12})1/2$ and $(1)3/2$ multiplets through in-plane components of AS exchange. It can be said that in-plane components of the AS exchange are reduced by the isotropic exchange so that under the realistic conditions $|D_n|, |D_{\perp}| \ll J$ the parameter $D_{\perp}$ is effectively small. At the same time this part of AS exchange leads to the avoided crossing of the magnetic sublevels of S=1/2 and S=3/2 multiplets in high field, at the crossing points the in-plane components of AS exchange act as a first order perturbation [36]. The excited $S = 3/2$ level shows also a zero-field splitting but this splitting $\Delta_1 = D_{\perp}^2/8J$ is not affected by the parameter D_n and represents solely a second order effect with respect to the in-plane part of AS exchange. For this reason the zero-field splitting of the excited quadruplet is expected to be smaller (if D_n and $D_{\perp}$ are comparable) than the splitting of two S=1/2 doublets. The sign of Δ determines the ground state, in the cases of $\Delta > 0$ and $\Delta < 0$ the ground states are the doublets with $|M_J| = 1/2$ and $|M_J| = 3/2$ respectively. The Zeeman sublevels are enumerated by the quantum number M_J as shown in Fig. 5 in the case of $\Delta > 0$, the fine structure of S=3/2 is shown in the inset. According to the general symmetry rule the levels with the same M_J show avoided crossing, meanwhile those with different M_J exhibit exact crossing (Fig. 3).

4. EPR TRANSITIONS, DISCUSSION OF EXPERIMENTAL DATA

Within the pseudoangular momentum approach one concludes that the general selection rule $M_J \to M_J \pm 1$ for the linearly polarized $\boldsymbol{H}_{osc} \perp C_3$ microwave field defines the allowed transitions as shown in Fig. 5. Using the analytical solutions for the Zeeman energies, one can evaluate the resonance fields for the EPR transitions. Recently we have reported [39] the representative schemes of transitions and EPR spectra simulated for different microwave

frequencies , included those used in the high-frequency EPR experiments at ultra-low temperatures [40]. In all calculations we used g=1.96 and $J = 0,847$ cm^{-1} that is consistent with the experimental data [41]. The zero-field splitting in the ground manifold $|\Delta|$ is set to 0.14 cm^{-1}, as was found from inelastic neutron scattering [11,12]. Since the normal and in-plane contributions of AS exchange can not be discriminated directly from the experimental data on the inelastic neutron scattering, the ratio $D_\perp/D_n$ is varied (providing fixed value of $|\Delta|$) in order to reveal the influence of different AS exchange components on the EPR pattern. The transformations of the spectrum with the increase of the ratio $D_\perp/D_n$ are also shown in the proposed EPR schemes [39] . We shall consider separately two cases: (*i*) $D_n \neq 0$, $D_\perp = 0$ and (*ii*) $D_n \neq 0$, $D_\perp \neq 0$. Since normal part of the AS exchange does not mix different spin levels one can discuss the case (*i*) within the Russel-Saunders scheme when the operator $\hat{S}_x$ does not change M_L. This implies the following selection rules for the linearly polarized microwave radiation that are strictly valid within the Russel-Saunders approximation: the EPR transitions $M_J \rightarrow M_J \pm 1$ are allowed with the conservation at the same time of the full spin S, projection of the orbital angular momentum M_L and for $M_S \rightarrow M_S \pm 1$ ($\Delta S = 0$, $\Delta M_L = 0$, $\Delta M_S = \pm 1$, $\Delta M_J = \pm 1$). The allowed intramultiplet transitions are schematically shown in Fig. 6 for three frequency domains: $h\nu < \Delta$, $\Delta < h\nu < 3J$ and $h\nu > 3J$. One can see that the spectrum consists of three lines, one line arises from three strong transitions **3, 4, 5** (marked bold) within S=3/2 multiplet with the resonance field $H_{\mathbf{3,4,5}} = h\nu/g\beta$ andthe two remaining lines correspond to two interdoublet transitions within two S=1/2 levels (Fig. 5, 6). It should be stressed that the intermultiplet ($S = 1/2 \leftrightarrow S = 3/2$) transitions are strictly forbidden when $D_\perp = 0$ as well as intradoublet transitions in the two S =1/2 levels split by AS exchange (this has been proved in [23–27]).

Two situations $h\nu < \Delta$ and $h\nu > \Delta$ within the case (*i*) are to be distinguished. Providing $h\nu < \Delta$ (Fig. 6a) two interdoublet transitions **1** and **1′** have the resonance fields $H_{\mathbf{1'}} = \left(\sqrt{3}D_n - h\nu\right)/g\beta$ and $H_{\mathbf{1}} = \left(\sqrt{3}D_n + h\nu\right)/g\beta$, so that the separation between these lines $H_{\mathbf{1}} - H_{\mathbf{1'}} = 2h\nu/g\beta$ increases with increase of the microwave frequency. The full spectrum is asymmetric with the line at $H_{\mathbf{3,4,5}} = h\nu/g\beta$ being closer to the line at $H_{\mathbf{1'}}$, the difference in the resonance fields $H_{\mathbf{1}} - H_{\mathbf{3,4,5}} = \sqrt{3}D_n/g\beta$ is independent of microwave frequency ν and $H_{\mathbf{1'}} - H_{\mathbf{3,4,5}} = \left(2h\nu - \sqrt{3}D_n\right)/g\beta$ increases with the increase of ν. At relatively high temperatures (when the full intensity follows the low $I \propto T^{-1}$) the ratio of the intensities of three lines is 1:3:1. In the case of $h\nu < \Delta$ the interdoublet transitions are **1**, **2** (Figs. 6b and 6c) with the resonance fields $H_{\mathbf{1}} = \left(h\nu + \sqrt{3}D_n\right)/g\beta$ and $H_{\mathbf{2}} = \left(h\nu - \sqrt{3}D_n\right)/g\beta$. In this case the spectrum consists of the central peak at $H_{\mathbf{3,4,5}} = \sqrt{3}D_n/g\beta$ and two equally spaced side-lines at $H_{\mathbf{1}}$ and $H_{\mathbf{2}}$ with the ratio intensities 1:3:1. It is remarkable that in the case under consideration the full width of the spectrum $H_{\mathbf{1}} - H_{\mathbf{2}} = 2\sqrt{3}D_n/g\beta$ is directly related to the AS exchange and independent of ν.

In the general case (*ii*) when both components of AS exchange are nonzero ($D_n \neq 0$ $D_t \neq 0$) different spin levels are mixed and the system can be adequately described by the *jj*-coupling scheme.Two new essential features of the EPR pattern arise from the mixing of S=1/2 and S=3/2 spin levels by the in-plane part of AS exchange. First, due to axial zero-field splitting $\Delta_1 = D_\perp^2/8J$ of the excited S=3/2 level the transitions **3, 4, 5** at $h\nu > \Delta_1$ have different resonance fields: $H_{\mathbf{3,5}} = \left(h\nu \mp \Delta_1\right)/g\beta$, $H_{\mathbf{4}} = g\beta$ and providing $h\nu < \Delta_1$ line **3** does not exist and line **5′** corresponds to $H_{\mathbf{5'}} = \left(\Delta_1 - h\nu\right)/g\beta$ (see Fig. 5, inset). This leads to a peculiar fine triplet structure of the central peak in the patterns of the EPR lines so far discussed. The second order effect of mixing through the in-plane AS exchange is relatively small in the wide range of the fields except of the vicinity of the avoided crossing points (Fig. 5) where the in-plane component of the AS exchange acts as a first order perturbation.

The second important consequence of the in-plane AS exchange is that this interaction allows new transitions (obeying the general selection rule $\Delta M_J = \pm 1$) that are forbidden in the Russel-Sauders scheme, namely, the

intermultiplet transitions 6-12 and 9′ as shown in Fig. 5. The intensities of these newly allowed transitions depend on the extent of the mixing of S=1/2 and S=3/2 multiplets in the magnetic field and in a wide range of the field they are relatively weak. The high-frequency ($\nu = 57.831 \text{GHz}$ and $\nu = 108 \text{ GHz}$) EPR measurements at ultra-low temperatures between 0.5 and 4.2K for the parallel ($\boldsymbol{H} \| C_3$) field have been recently reported [42]. The transmission spectrum observed at 2.1T represents a relatively broad slightly asymmetric peak that becomes broader when the temperature decreases (Fig. 7). Since the observed structureless EPR peak does not provide unambiguous information about the fine structure of the absorption we will discuss a simplest approximation in which only the normal part of the AS exchange is taken into account. Since the fine structure of the absorption line is unresolved it is
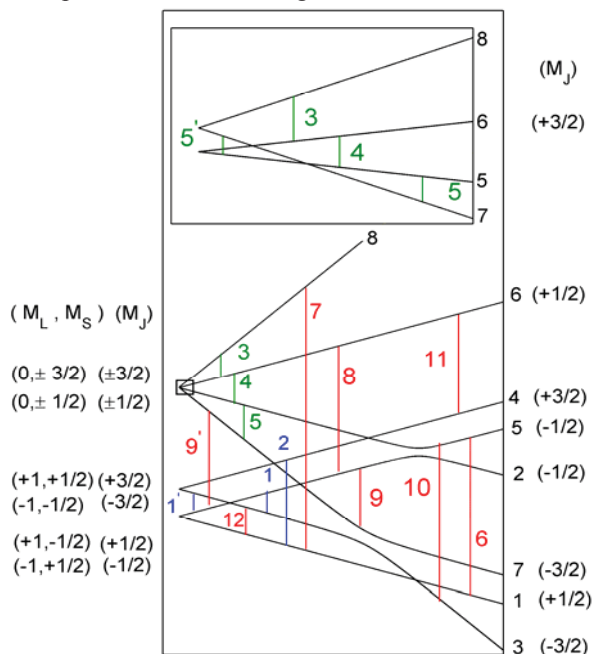
Fig. 5. Energy pattern of V_{15} molecule within the three-spin model $\left(\text{the case } \Delta > 0\right)$ and allowed EPR transitions in the parallel ($\boldsymbol{H} \| C_3$) field. Inset: magnified zero-field and Zeeman splitting of S=3/2 level ($\boldsymbol{H} \| C_3$).
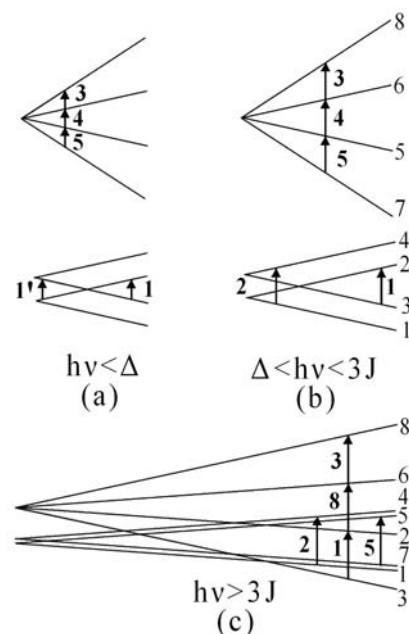
Fig. 6. Scheme of the EPR transitions in the case of $D_\perp = 0$: (a) $h\nu < \Delta$, (b) $h\nu > \Delta < 3J$, (c) $h\nu > 3J$.
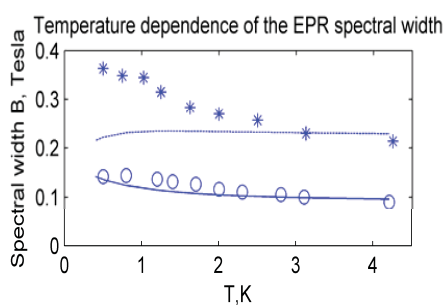
Fig. 7. Theoretical and experimental temperature dependence of the EPR spectral width for V_{15}. The theoretical curves are scaled at $T = 3K$, $J = 0.847 \ cm^{-1}$, $\Delta = 0.14 \ cm^{-1}$ ($\boldsymbol{H} \| C_3$). Theoretical curves: 57.831 GHz (solid), 108 GHz (dashed), experimental data: 57.831 GHz (circles) 108 GHz (stars).
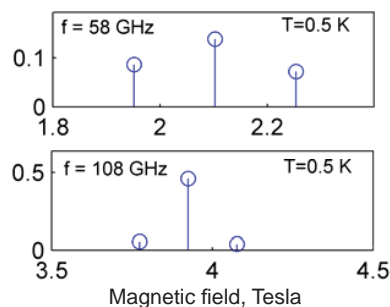
Fig. 8. Calculated EPR lines ($\boldsymbol{H} \| C_3$) at $T = 0.5K$ for two frequencies. ($J = 0.847 \ cm^{-1}$, $\Delta = 0.14 \ cm^{-1}$).

reasonable to assume that the observed peak can be considered as an envelope of the broadened individual absorption lines arising from the allowed transitions. In the case of $v = 57.831$ GHz (frequency region $\Delta < h\nu < 3J - \Delta/2$) the superposition involves the central lines **3,4,5** at $H_{3,4,5} = 2.11$T and two sidebands **1** and **2** at $H_1 = 1.96$T and $H_2 = 2.26$T. At the frequency $v = 108$ GHz the full spectrum is assumed to consist of the central peak **1,3,8** and sidelines **2** and **5** ($H_{1,3,8} = 3.93$T, $H_2 = 3.78$T and $H_5 = 4.08$T). In order to estimate approximately the role of the AS exchange in the broadening of the EPR peak we have calculated the central second moments of these discrete spectral distributions:

$$\left\langle \left(H - \overline{H}\right)^2 \right\rangle = \sum_{i=1}^{3} I_i \left(H_i - \overline{H}\right)^2 \Bigg/ \sum_{i=1}^{3} I_i , \tag{5}$$

where I_i are the intensities of the lines at a given temperature and $\overline{H}$ is the center of the first moment (center of gravity) of the spectral distribution:

$$\overline{H} = \sum_{i=1}^{3} I_i H_i \Bigg/ \sum_{i=1}^{3} I_i . \tag{6}$$

where I_i are the intensities of the lines at a given temperature and $\overline{H}$ is the center of the first moment (center of gravity) of the spectral distribution. The full with of the observed peak includes also contributions arising from the broadening of the individual lines. In order to take them into account, at least qualitatively, we have normalized the full width (obtained with the aid of Eqs. (5) and (6)) vs. temperature at $T = 3K$. As one can see the evaluated temperature dependence of the spectral width is in reasonable agreement with the experimental data at $v = 57.831$GHz (Fig. 6). At the same time at $v = 108$ GHz probably the splitting of the lines due to AS exchange plays a secondary role in the broadening of the observed EPR peak, especially at ultra-low temperatures. This can be also be illustrated by plotting of the EPR pattern at $T = 0.5$ K for two employed frequencies (Fig. 8). One can see that at low temperature the second moment at $v = 108$ GHz is less than that for $v = 57.831$ GHz due to lower intensity of the sidebands meanwhile the

observed width is greater. Calculations of the second moments in a more general model when $D_\perp \neq 0$ give similar results but the smoothed line does not provide a reliable information about the interrelation between two components of AS exchange. In view of these results one might assume that the broadening of the EPR peak can be attributed to the spin-phonon interaction and also to the effects of lower symmetry that have been recently discussed [19]. More detailed information can be provided by the angular dependence of the high-frequency EPR and by the study of the mechanisms of relaxation. The hyperfine interaction is to be mentioned as an essential contribution to the broadening of the EPR line in the vanadium clusters.

5. ZEEMAN LEVELS IN PERPENDICULAR FIELD

In the important particular case when the in-plane of AS exchange is absent $\left(D_n \neq 0, D_l = D_t = 0\right)$ the special symmetry properties of the matrix of AS exchange do allow to find the exact solution:

$$\varepsilon_1 = \varepsilon_3 = -\frac{3}{2}J - \frac{1}{2}\sqrt{\left(g\beta H\right)^2 + 3D_n^2} \ ,$$

$$\varepsilon_2 = \varepsilon_4 = -\frac{3}{2}J + \frac{1}{2}\sqrt{\left(g\beta H\right)^2 + 3D_n^2} \ ,$$

$$\varepsilon_{5,6} = \frac{3}{2}J \mp \frac{1}{2}g\beta H \ , \tag{7}$$

$$\varepsilon_{7,8} = \frac{3}{2}J \mp \frac{3}{2}g\beta H \ .$$

In Eq. (7) H is the field in any direction in the plane, let say $H = H_X$ and correspondingly g-factor $g \equiv g_\perp$. The levels ε_i (H) with $i = 1, 2, 3, 4$ are related to $S=1/2$ while $i=5,6,7,8$ are the numbers of Zeeman sublevels for $S=3/2$ (with $M = \mp 1/2$ and $M = \mp 1/2$) as shown in Fig. 9a in the case of the isotropic model. The energy pattern for the case

$D_n \neq 0$, $D_l = D_t = 0$ is shown in Fig. 9b. Three peculiarities of the energy pattern that are closely related to the magnetic behavior should be noticed: 1) the ground state involving two $S = 1/2$ levels shows zero-field splitting into two Kramers doublets separated by the gap $\Delta = \sqrt{3}D_n$; 2) at low fields $g\beta H \leq \Delta$ the Zeeman energies are double degenerate and show quadratic dependence on the field:

$$\varepsilon_1 = \varepsilon_3 = -\sqrt{3}D_n \big/ 2 - \left(g\beta H\right)^2 \big/ 4\sqrt{3}D_n,$$

$$\varepsilon_2 = \varepsilon_4 = -\sqrt{3}D_n \big/ 2 + \left(g\beta H\right)^2 \big/ 4\sqrt{3}D_n. \tag{8}$$

This behavior is drastically different from that in the isotropic model and from the linear magnetic dependence in parallel field [23] and can be considered as a breaking of the normal AS exchange by the perpendicular field [23]; 3) the magnetic sublevels arising from $S = 3/2$ ($M = -1/2$ and $M = -3/2$) cross the sublevels belonging to $S = 1/2$ spin levels, no avoided crossing points are observed. At high field the levels $\varepsilon_{1,3}$ and $\varepsilon_{2,4}$ exhibit again linear magnetic dependence. One can see that strong perpendicular field restores linear Zeeman splitting but without zero-field splitting so that the perpendicular field reduces the normal part of AS coupling. This effect of reduction has been understood long time ago [23].

When the AS exchange in its general form is involved $\left(D_n \neq 0, D_l \neq 0, D_t \neq 0\right)$ the energy pattern shows new peculiarities (Fig. 9c). The low field part of the spectrum is not affected by the in-plane part of AS exchange and is very close to that in Fig. 9b due to the fact that the in-plane part of AS exchange is not operative within the ground manifold and the effect of $S = 1/2$-$S = 3/2$ mixing is small at low fields due to the large gap $3J \gg |D_\perp|$. At the same time in the vicinity of the crossing points the effect of the normal AS exchange is negligible but the in-plane AS exchange acts as a first order perturbation giving rise to the avoided crossings as shown in Fig. 9c.

Let us note that at low fields far from anticrossing region the energies can be well described by the Eq. (8) in general case of AS exchange although they are deduced for a particular model when $\left(D_n \neq 0, D_l \neq 0, D_t \neq 0\right)$. In order to obtain three closely spaced low lying levels in the region of anticrossing field we will use the perturbation theory respectively to the in-plane part of AS exchange and the basis formed by three eigen-functions of H_0 whose eigen-values have crossing point at $g\beta H = 3J$, namely $\left|(0)1/2, -1/2\right\rangle, \left|(1)1/2, -1/2\right\rangle, \left|(1)3/2, -3/2\right\rangle$ (Fig. 9a). The secular equation can be solved due to some additional symmetry. The following approximate expressions were found [43,44] for the energy levels ε_i' in this region of the field:

$$\varepsilon_1' = -\frac{3}{2}J - \frac{1}{2}g\beta H, \tag{9}$$

$$\varepsilon_{3,7}' = -g\beta H \mp \frac{1}{8}\sqrt{\left(4g\beta H - 12J\right)^2 + 18D_\perp^2}, \tag{10}$$

These expressions give rather good accuracy and will be used in the description of the magnetization vs. field and temperature of V_{15} cluster.

6. TEMPERATURE AND FIELD DEPENDENCE OF MAGNETIZATION OF V_{15} -EFFECTS OF AS EXCHANGE

Let us consider some general features of the field dependence of magnetization related to the AS exchange by plotting the results of sample calculations. The most spectacular is the low molecule) that work well at low field (Eq. (11)) and high field in the vicinity of anticrossing of the low lying levels (Eq. (12)) :

$$\mu(H) = \frac{g^2\beta^2 H}{2\sqrt{3D_n^2 + g^2\beta^2 H^2}}, \tag{11}$$

$$\mu(H) = g\beta + \frac{2g\beta\left(g\beta H - 3J\right)}{\sqrt{2\left(g\beta H - 3J\right)^2 + 18D_\perp^2}}. \tag{12}$$

Fig.9 (dashed line) shows $\mu(H)$ dependence in the framework of the isotropic model. The normal part of AS exchange results in the broadening of the low field step in $\mu(H)$ as shown by solid line. This broadening is closely related to the quadratic Zeeman effect in the low perpendicular field (see Fig. 9b). The in-plane part of the AS exchange leads to the broadening of the second step. When anticrossing in the region $H = 3J/g\beta$ appears due
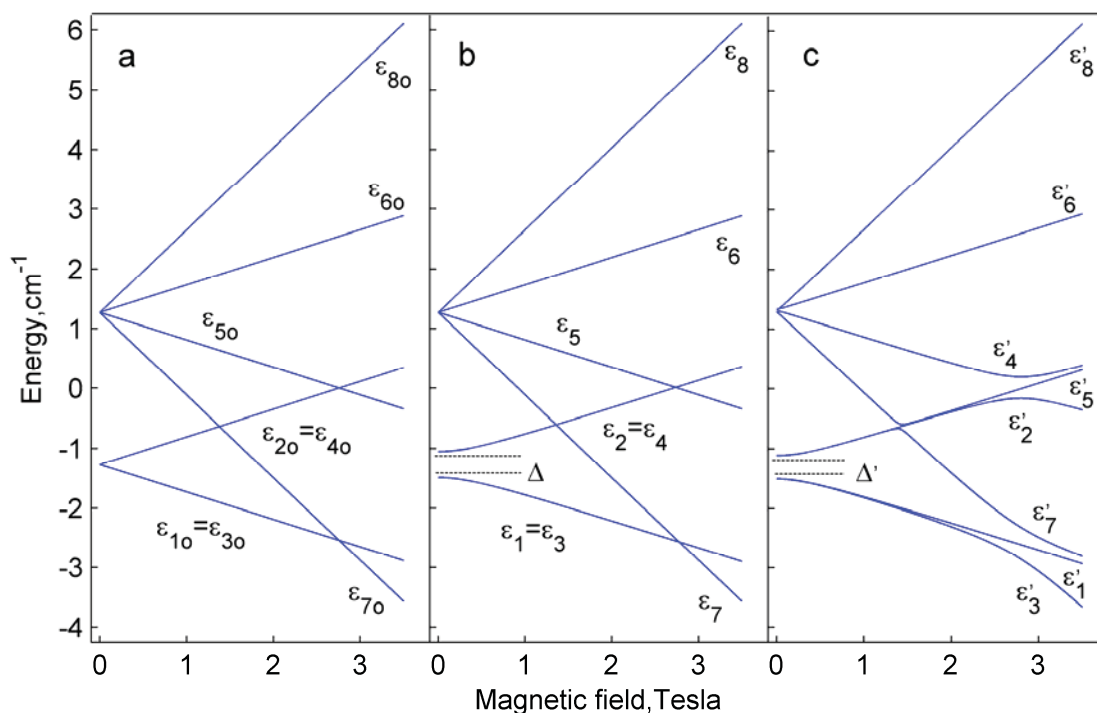
Fig. 9. Energy pattern of the triangular vanadium unit in the magnetic field applied in the plane ($\boldsymbol{H} \perp C_3$),

$$J = 0.847 \, cm^{-1}, g = 2. \quad \text{(a)} \ D_n = 0, \ D_\perp = 0; \text{(b)} \ D_n = 0.3J, D_\perp = 0,$$

$$\text{(c)} \ D_n = 0.3J, \ D_\perp = 0.6J.$$

coupling of S=1/2, M=-1/2 S=3/2, M=-3/2 levels through in-plane AS exchange it obviously gives rise to a smoothed switch from S=1/2 to S=3/2 as shown in Fig. 9c. Fig. 10 schematically indicates that the first and the second steps of magnetization are affected by the two different parts of the AS exchange.

7. TEMPERATURE AND FIELD DEPENDENCE OF MAGNETIZATION - DISCUSSION OF EXPERIMENTAL DATA

The low-temperature adiabatic magnetization vs. field applied in the plane of the V_3 triangle ($\boldsymbol{H} \perp C_3$) exhibits steps whose broadening and shapes are temperature dependent (Figs. 10,11). Analysis of the experimental data in [41] has been performed in the framework of the HDVV model supplemented by a small quadrupolar anisotropy $\left(J_{XX} = J_{YY} \neq J_{ZZ}\right)$. Agreement between the calculated curves and experimental magnetization data proved to be quite good for T= 0.9 K and 4.2 K but the model fails to explain the low temperature data.

Modeling magnetization curves with consideration of the AS exchange gives perfect agreement for the whole range of temperatures including the lowest one. Such a modeling for the first time allowed us to estimate the AS exchange parameters. The best fit procedure gives the following set of parameters: $J = -0.855 cm^{-1}$, $g = 1.94$, $D_\perp = 0.238 \, cm^{-1}$, $D_n = 0.054 \, cm^{-1}$ (see [43,44]). The least mean square error value calculated for the whole sets

of the $\mu(H)$ curves is found to be $2.3 \cdot 10^{-3}$. The fit is well stable for the parameters *J*, *g* and $D_\perp$ but however, less stable with respect to D_n (see [44] for more details). To determine this parameter more accurately one needs low field
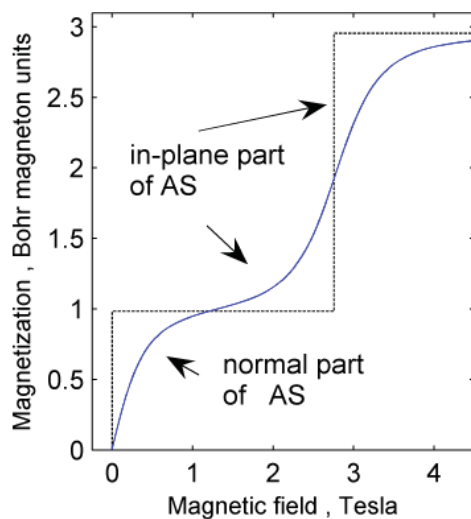
Fig. 10. Magnetization at T = 0 K
in perpendicular field.
Dashed line : $J = 0.847 \ cm^{-1}$,
$D_n = 0$, $D_\perp = 0$;
Solid line: $J = 0.847 \ cm^{-1}$,
$D_n = 0.3J$, $D_\perp = 0.6J$.
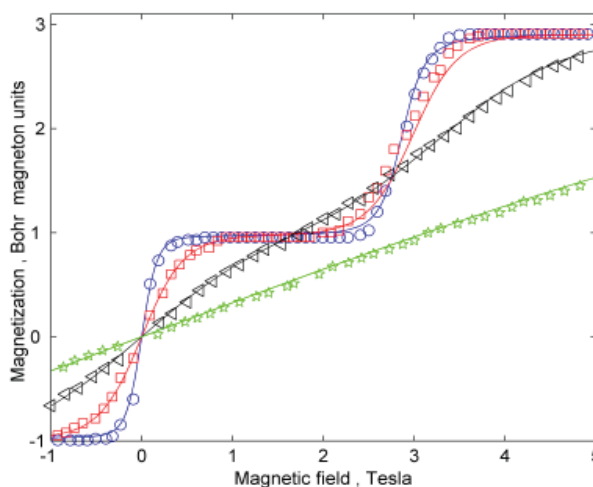
Fig.11. Experimental data (from ref [41])
and theoretical curves of static magnetization
calculated with account for the isotropic
and AS exchange interactions ($\boldsymbol{H} \perp C_3$).
Experimental data : Circles- $T = 0.1 \ K$,
squares- $T = 0.3K$, triangles- $T = 0.9 \ K$,
stars– $T = 4.2 \ K$. Solid lines- calculated.

data at ultra-low temperatures and additional data like EPR at low frequencies. Calculated curves (with the best fit parameters) and experimental data are in full agreement in the whole ranges of the temperature and field used in the experiments so far mentioned (Fig. 11).

8. VIBRONIC INTERACTION

Since the exchange multiplets are orbitally degenerate the role of the vibronic coupling (Jahn-Teller-JT-effect [45-47]) should be elucidated. We will use the semiclassic adiabatic approximation that gives clear physical picture of the influence of the vibronic interaction on the magnetic characteristics. In the JT systems, in general, the electronic and vibrational states are mixed [45-47]. Nevertheless, in many important cases the adiabatic approach can serve as a relatively simple and at the same time powerful tool for the theoretical study of the JT systems. The question of the applicability of the semiclassic adiabatic approach to the vibronic problems in the JT systems is rather complicated in general (and will not be discussed here) and the thorough answer can be done with regard to a particular problem. The results of the semiclassic calculations of the magnetic moments in pseudo JT (mixed-valence) clusters vs. temperature were carefully tested by comparison with the results of quantum-mechanical evaluation [48]. The results exhibit very high accuracy of the semiclassic theory in a wide range of the temperature and coupling parameters including cases of intermediate and even weak coupling. The qualitative difference in the estimation of magnetic behavior between the semiclassic and dynamic approaches was intentionally found for a specific choice of the parameters when the ground vibronic levels belonging to different spin values are close. This conclusion is common for the thermodynamic (non-resonance) characteristics of the JT systems that are defined exceptionally by the partition function. Keeping in mind these results, in the present study we shall take advantage of the semiclassic adiabatic approach in order to reveal the influence of the vibronic coupling on magnetization in the presence of the AS exchange.

The symmetry adapted vibrations $A_1\left(Q_{A_1} \equiv Q_1\right)$ and double degenerate *E* type $\left(Q_{Ex} \equiv Q_x, Q_{Ey} \equiv Q_y\right)$ of an equilateral triangular unit can be expressed as

$$Q_1 = \tfrac{1}{\sqrt{3}}\left[-\tfrac{1}{2}\left(\sqrt{3}X_1 + Y_1\right) + \tfrac{1}{2}\left(\sqrt{3}X_2 - Y_2\right)\right],$$

$$Q_x = \tfrac{1}{\sqrt{3}}\left[-\tfrac{1}{2}\left(\sqrt{3}X_1 - Y_1\right) - \tfrac{1}{2}\left(\sqrt{3}X_2 + Y_2\right)\right],$$

$$Q_y = \tfrac{1}{\sqrt{3}}\left[\tfrac{1}{2}\left(X_1 + \sqrt{3}Y_1\right) + \tfrac{1}{2}\left(X_2 - \sqrt{3}Y_2\right) - X_3\right]. \tag{13}$$

The vibronic interaction arises from the modulation of the isotropic and AS exchange interactions by the molecular displacements. In fact, the exchange parameters are the functions of the interatomic distances so the linear terms of the vibronic Hamiltonian can be represented as:

$$H_{ev} = 2\sum_{ij} \mathbf{S}_i \mathbf{S}_j \sum_{\alpha=1,x,y} \left(\frac{\partial J_{ij}(R_{ij})}{\partial R_{ij}}\right)_{\Delta R_{ij}=0} \cdot \frac{\partial R_{ij}}{\partial Q_\alpha} Q_\alpha, \tag{14}$$

$$H'_{ev} = \sum_{ij}[\mathbf{S}_i \times \mathbf{S}_j] \sum_{\alpha=1,x,y} \left(\frac{\partial \mathbf{D}_{ij}(R_{ij})}{\partial R_{ij}}\right)_{\Delta R_{ij}=0} \cdot \frac{\partial R_{ij}}{\partial Q_\alpha} Q_\alpha \tag{15}$$

Here the summation is extended over all pairwise spin-spin interactions (ij= 12, 23, 31). Eqs. (14) and (15) are the contributions of the overall vibronic coupling relating to the isotropic and AS exchange interactions respectively. After all required transformations one can arrive at the following vibronic Hamiltonian H_{ev}:

$$H_{ev} = \lambda\left(\hat{V}_1 Q_1 + \hat{V}_x Q_x + \hat{V}_y Q_y\right) \tag{16}$$

where $\lambda \equiv \sqrt{6}\left(\partial J_{ij}(R_{ij})/\partial R_{ij}\right)_0$ is the vibronic coupling parameter associated with the isotropic exchange and the operators $\hat{V}_\alpha$ are the following [49] (see [23,27] and references cited therein):

$$\hat{V}_1 = \sqrt{\tfrac{2}{3}}\left(\mathbf{S}_1 \mathbf{S}_2 + \mathbf{S}_2 \mathbf{S}_3 + \mathbf{S}_3 \mathbf{S}_1\right), \tag{17}$$

$$\hat{V}_x = \tfrac{1}{\sqrt{6}}\left(\mathbf{S}_2 \mathbf{S}_3 + \mathbf{S}_3 \mathbf{S}_1 - 2\mathbf{S}_1 \mathbf{S}\right),$$

$$\hat{V}_y = \tfrac{1}{\sqrt{2}}\left(\mathbf{S}_2 \mathbf{S}_3 - \mathbf{S}_3 \mathbf{S}_1\right).$$

By applying a similar procedure one can obtain the vibronic contribution associated with the AS exchange. The final expression is the following:

$$H'_{ev} = \hat{W}_1 Q_1 + \hat{W}_x Q_x + \hat{W}_y Q_y. \tag{18}$$

The operators $\hat{W}_\alpha$ are expressed in terms of the vector products of spin operators:

$$\hat{W}_1 = \lambda_{12}[\mathbf{S}_1 \times \mathbf{S}_2] + \lambda_{23}[\mathbf{S}_2 \times \mathbf{S}_3] + \lambda_{31}[\mathbf{S}_3 \times \mathbf{S}_1],$$

$$\hat{W}_x = \tfrac{1}{2}\left(\lambda_{12}[\mathbf{S}_1 \times \mathbf{S}_2] + \lambda_{23}[\mathbf{S}_2 \times \mathbf{S}_3] - 2\lambda_{31}[\mathbf{S}_3 \times \mathbf{S}_1]\right),$$

$$W_y = \tfrac{\sqrt{3}}{2}\left(\lambda_{23}[\mathbf{S}_2 \times \mathbf{S}_3] - \lambda_{31}[\mathbf{S}_3 \times \mathbf{S}_1]\right). \tag{19}$$

In Eq. (19) the values λ_{ij} are the vector coupling parameters defined as $\lambda_{ij} = \left(\partial \mathbf{D}_{ij}(R_{ij})/\partial R_{ij}\right)_0$. Under the condition of trigonal symmetry there are three parameters, namely, normal part $\lambda_n = \lambda_{ijn}$ and two perpendicular contributions $\lambda_t = \lambda_{ijt}$ and $\lambda_l = \lambda_{ijl}$ where the symbols l and t have the same meaning as in the definition of the AS exchange. As one can see the vibronic interaction appears due to dependence of the exchange parameters (isotropic and anisotropic)

upon the distances between the metal centers that means that the physical origin of the vibronic (or spin-vibronic) interaction is the modulation of the exchange interaction by the molecular or lattice vibrations. This leads to the fact that the matrix elements of the spin-vibronic interactions are expressed in terms of the two-particle operators. This is in line of the traditional theory of the JT effect but takes into account the feature of the exchange coupled systems. If an irrelevant *ab-initio* scheme for the evaluation of the exchange parameters as the functions of the distances is employed the corresponding derivatives (Eqs. (14) and (15)) with respect to the metal-metal distances can be calculated.

The evaluation of the vibronic matrices can be performed with the aid of the ITO approach [27, 38,50]. With this aim each pairwise interaction can be expressed in terms of the zeroth order and first order tensorial products of ITOs as:

$$\left(S_i\, S_j\right) = -\sqrt{3}\left\{S_i^{(1)} \times S_j^{(1)}\right\}^{(0)},\tag{20}$$

$$\lambda_{ij}\left[S_i \times S_j\right] = i\sqrt{2}\,\lambda_-\,e^{-i\phi}\left\{S_i^{(1)} \times S_j^{(1)}\right\}_1^{(1)} - i\sqrt{2}\,\lambda_+\,e^{i\phi}\left\{S_i^{(1)} \times S_j^{(1)}\right\}_{-1}^{(1)} - i\sqrt{2}\,\lambda_n\left\{S_i^{(1)} \times S_j^{(1)}\right\}_0^{(1)}$$

where $\left\{S_i^{(1)} \times S_j^{(1)}\right\}_m^{(k)}$ is the symbol of the tensor product [50] (rank κ, component m) of two spin ITOs $S_i^{(1)}$ and $S_j^{(1)}$ relating to the sites i and j and $\phi = 0,\ 2\pi/3,\ 2\pi/3$ for the sides 12, 23 and 31 of the triangle correspondingly,

$$\lambda_{\pm} = \mp\left(1/\sqrt{2}\right)\left(\lambda_l \pm i\lambda_t\right).$$

8. VIBRONIC MATRIX FOR THE GROUND STATE AND ADIABATIC SURFACES

In order to simplify our consideration and to get clear insight on the influence of the JT interaction on the magnetic properties we assume that the gap 3J exceeds considerably the vibronic coupling and AS exchange and therefore we include in the basis set only four low laying spin 1/2 states and exclude the full symmetric mode Q_1. In this view one should note that the role of A_1 mode is not a simple shift of Q_1 the coordinate. In fact, A_1 vibration is active in the pseudo JTE when a relatively small vibronic contribution of AS exchange is taken into account (a more detailed description will be given elsewhere). In the approximation so far assumed the matrix of the full Hamiltonian

$$H_{AS} + H_{ev} + H'_{ev} + H_{Zeeman}\quad \text{was obtained in [51]:}$$

$$\begin{pmatrix} \frac{1}{2}g_{||}\beta H_z + \frac{1}{2}\sqrt{\frac{3}{2}}\lambda Q_x & \frac{1}{2}g_\perp\beta H_x & \frac{\sqrt{3}}{2}\left(-iD_n + \frac{1}{\sqrt{2}}\lambda Q_y\right) & \frac{i}{2}\sqrt{\frac{3}{2}}\lambda_-\left(Q_x + iQ_y\right) \\ \frac{1}{2}g_\perp\beta H_x & -\frac{1}{2}g_{||}\beta H_z + \frac{1}{2}\sqrt{\frac{3}{2}}\lambda Q_x & -\frac{i}{2}\sqrt{\frac{3}{2}}\lambda_+\left(Q_x - iQ_y\right) & \frac{\sqrt{3}}{2}\left(iD_n + \frac{1}{\sqrt{2}}\lambda Q_y\right) \\ \frac{\sqrt{3}}{2}\left(iD_n + \frac{1}{\sqrt{2}}\lambda Q_y\right) & -\frac{i}{2}\sqrt{\frac{3}{2}}\lambda_-\left(Q_x + iQ_y\right) & \frac{1}{2}g_{||}\beta H_z - \frac{1}{2}\sqrt{\frac{3}{2}}\lambda Q_x & \frac{1}{2}g_\perp\beta H_x \\ -\frac{i}{2}\sqrt{\frac{3}{2}}\lambda_+\left(Q_x - iQ_y\right) & \frac{\sqrt{3}}{2}\left(-iD_n + \frac{1}{\sqrt{2}}\lambda Q_y\right) & \frac{1}{2}g_\perp\beta H_x & -\frac{1}{2}g_{||}\beta H_z - \frac{1}{2}\sqrt{\frac{3}{2}}\lambda Q_x \end{pmatrix}\tag{21}$$

In the matrix representation of the full Hamiltonian the basis $\left|(S_{12})SM\right\rangle$ is used with the following order of the basis spin functions: $\left|(0)\frac{1}{2},\frac{1}{2}\right\rangle, \left|(0)\frac{1}{2},-\frac{1}{2}\right\rangle, \left|(1)\frac{1}{2},\frac{1}{2}\right\rangle, \left|(1)\frac{1}{2},-\frac{1}{2}\right\rangle$. Since the system has axial magnetic anisotropy one can that the field is applied in a ZX plane ($H_y = 0$). One sees that the vibronic interaction leads to a complicated combined JT and pseudo JT problem. The modulation of the isotropic exchange is expected to provide the dominant contribution to the vibronic interaction. To further simplify the solution of the problem and make it more obvious we put $\lambda_+ = \lambda_- = 0$ and $g_{||} = g_\perp = g$ (although the eigen-values of the vibronic matrix are found without these simplifying assumptions). The four eigen-values of the matrix are found as:

$$\varepsilon_{1,4}(\rho,\xi) = \mp \frac{1}{2\sqrt{2}} \hbar\omega \sqrt{2\xi^2 + 2\delta^2 + 3\upsilon^2\rho^2 - 2\sqrt{2}\,\xi\sqrt{3\upsilon^2\rho^2 + 2\delta^2 \cos^2\theta}}$$

$$\varepsilon_{2,3}(\rho,\xi) = \pm \frac{1}{2\sqrt{2}} \hbar\omega \sqrt{2\xi^2 + 2\delta^2 + 3\upsilon^2\rho^2 + 2\sqrt{2}\,\xi\sqrt{3\upsilon^2\rho^2 + 2\delta^2 \cos^2\theta}} \qquad (22)$$

The following dimensionless parameters are introduced: vibronic coupling parameter $\upsilon = (\lambda/\hbar\omega)(\hbar/M\omega)^{1/2}$, zero field splitting of the ground state $\delta = \sqrt{3}D_n/\hbar\omega \equiv D/\hbar\omega$, applied field $\xi = g\beta H/\hbar\omega$ and the vibrational coordinates $q_\alpha = (M\omega/\hbar)^{1/2} Q_\alpha$, the angle θ is defined by $H_z = H\cos\theta$. Finally, ρ is the radial component in the plane $q_x\,q_y$ defined as usually: $q_x = \rho\cos\varphi$, $q_y = \rho\sin\varphi$. The adiabatic surfaces are axially symmetric (at an arbitrary direction of the applied field) respectively the C_3 axis complying with the actual axial symmetry of the AS exchange.

In the case of $\delta = 0$ and $\xi = 0$ one faces a two mode pseudo JT problem and one obtains simple expressions for a pair of the double degenerate surfaces that are quite similar to that in the pseudo JT $^2E \otimes e$ problem with spin-orbital interaction:

$$U_\pm(\rho)/\hbar\omega = \frac{\rho^2}{2} \pm \frac{1}{2}\sqrt{\delta^2 + \frac{3\upsilon^2\rho^2}{2}}. \qquad (23)$$

One can see that in the limit of the isotropic exchange model the surface represents a "Mexican hat" (Fig. 12a) with the
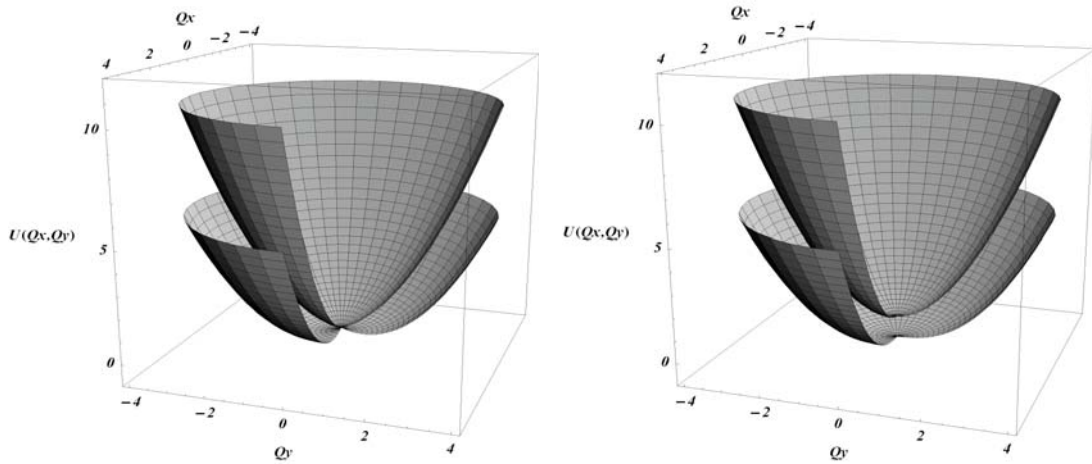
Fig. 12. Adiabatic potentials for the ground state of a triangular exchange system in the space of the double degenerate vibrations: (a) $\delta = 0, \upsilon = 2.0$; (b) strong AS exchange and/or weak vibronic interaction ($\delta = 1.0, \upsilon = 1.0$).
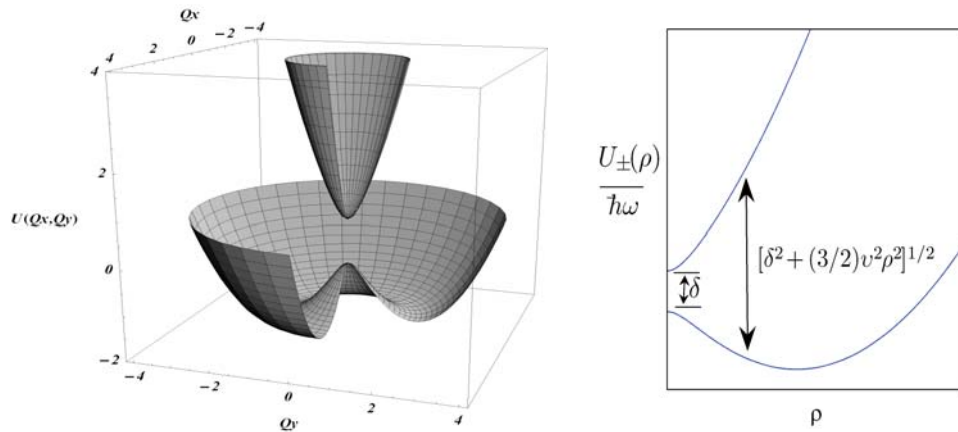
Fig. 13. The case of weak AS exchange and/or strong vibronic interaction ($\delta = 1.0, \upsilon = 3.0$).

Section of the adiabatic potentials in the case of JT instability, illustration for the zero-field splitting of the ground state in the vibronically distorted configurations conical intersection at $\rho = 0$ that corresponds to the basic JT $E \otimes e$ problem [23-25]: $U_\pm(\rho)/\hbar\omega = \rho^2/2 \pm (\sqrt{3}/2\sqrt{2})|\upsilon|\rho$. This limiting case corresponding to the well known spin-phonon coupling Hamiltonian [49] (see for details [23, 27] and references cited therein) has recently been considered again in [48]. In general, the shape of the surfaces depends on the interrelation between the AS exchange and vibronic coupling that proved to be competitive. In the case of weak vibronic coupling and/or strong AS exchange $\upsilon^2 < 4|\delta|/3$ the lower surface possesses the only minimum at $q_x = q_y = 0 (\rho = 0)$ so that the symmetric (trigonal) configuration of the system proves to be stable. In the opposite case of strong vibronic interaction and/or weak AS exchange, $\upsilon^2 > 4|\delta|/3$, symmetric configuration of the cluster is unstable and the minima are disposed at the ring of the trough of the radius ρ_0:

$$\rho_0 = \frac{1}{2}\sqrt{\frac{3\upsilon^2}{2} - \frac{8\delta^2}{3\upsilon^2}} .$$

The radius ρ_0 decreases with the increase of AS exchange and vanishes at $|\delta| = 3\upsilon^2/4$ (defining thus critical value of the vibronic coupling υ_0). Example of this type of the pseudo JT surfaces is shown in Fig. 12b. The depth of the minima ring in the second type (respectively to the top in the low surface) depends on the interrelation between the JT constant and AS exchange and is found to be $\varepsilon_0 = (3\upsilon^2 - 4\delta^2)^2/48\upsilon^2$ while the gap between the surfaces in the minima points $3\upsilon^2/4$ is independent of the AS exchange. Fig. 13 shows the case of strong JT coupling (instability) and the cross-section of the adiabatic potentials.

10. INFLUENCE OF THE JAHN-TELLER EFFECT ON THE MAGNETIZATION

To clarify the physical situation let us assume that the motion of the system is confined to the bottom of the trough. Strictly speaking this is valid providing strong JT coupling but in all cases it gives clear qualitative results and transparent key expressions keeping at the same time good accuracy in the quantitative description. Providing $\rho = \rho_0' \equiv \sqrt{3/8}\,|\upsilon|$ (radius of the minima ring) the value $\sqrt{3\upsilon^2\rho^2/2}$ is simply the JT splitting $E_{JT} = 3\upsilon^2/4$ (gap between the surfaces in the minima points of the lower surface) one obtains for the Zeeman sublevels in the weak field range up to the second order terms with respect to the field ξ defined by the angle θ can be found as:

$$\frac{\varepsilon_{1,3}(\xi)}{\hbar\omega} = -\frac{1}{2}\delta(\rho_0') \pm \frac{1}{2}\kappa_1(\theta)\xi - \kappa_2(\theta)\xi^2 ,$$

$$\frac{\varepsilon_{2,4}(\xi)}{\hbar\omega} = +\frac{1}{2}\delta(\rho_0') \pm \frac{1}{2}\kappa_1(\theta)\xi + \kappa_2(\theta)\xi^2 .$$

(24)

where the eigen-values are denoted as $\varepsilon_i(\xi) \equiv \varepsilon_i(\rho_0', \xi)$ and the van Vleck coefficients $\kappa_1(\theta)$ (first coefficient) and $\kappa_2(\theta)$ (second coefficient) [53] can be directly related to the JT splitting and AS exchange by:

$$\kappa_1(\theta) = \sqrt{\frac{E_{JT}^2 + \delta^2\cos^2\theta}{E_{JT}^2 + \delta^2}} ,$$

$$\kappa_2(\theta) = \frac{\delta^2\sin^2\theta}{4(E_{JT}^2 + \delta^2)^{3/2}} .$$

(25)

In order to reveal the influence of the JT coupling on the anisotropic properties of the AS exchange in more detail let us consider the effects of JT coupling in the two principal directions of the magnetic field. In the case of parallel field ($H \| C_3$) one finds that $\kappa_1(0) = 1$ and $\kappa_2(0) = 0$ so that one obtains the linear Zeeman splitting in a pair of spin doublets in the parallel field but the role the zero-field splitting plays now the combined effective gap $\sqrt{E_{JT}^2 + \delta^2}$ instead of the initial one $|\delta|$ related to the AS exchange. In the case of perpendicular field $H \perp C_3$ one obtains:

$$\frac{\varepsilon_{2,4}(\xi)}{\hbar\omega} = +\frac{1}{2}\sqrt{E_{JT}^2 + \delta^2} \pm \frac{E_{JT}}{\sqrt{E_{JT}^2 + \delta^2}} \frac{1}{2}\xi + \frac{\delta^2}{4\left(E_{JT}^2 + \delta^2\right)^{3/2}} \xi^2 \,.$$

(26)

Eq. (26) show that the Zeeman pattern contains both linear and quadratic contributions. The role of the JT coupling can be understood by comparing the Zeeman picture so far obtained with that at $\upsilon = 0$. It is important that in the absence of the JT coupling the linear Zeeman terms disappear and the Zeeman energies contain only quadratic terms (with respect to the field). Thus Fig. 14a illustrates two degenerate pairs of the Zeeman levels in perpendicular field in the symmetric nuclear configuration. In a weak field range they are given by:

$$\frac{\varepsilon_1(\xi)}{\hbar\omega} = \frac{\varepsilon_3(\xi)}{\hbar\omega} = -\frac{|\delta|}{2} - \frac{\xi^2}{4|\delta|} \quad , \quad \frac{\varepsilon_2(\xi)}{\hbar\omega} = \frac{\varepsilon_4(\xi)}{\hbar\omega} = +\frac{|\delta|}{2} + \frac{\xi^2}{4|\delta|} .$$

(27)

This can be referred to as the effect of the reduction of the magnetization in low magnetic field that is perpendicular to the axis of AS exchange [23,27]. The reduction of the Zeeman energy by the AS exchange gives rise to a small van Vleck type contribution to the magnetic susceptibility at low field $g\beta H \ll D_n$. An essential effect is that the JT interaction leads to the occurrence of the linear terms for the Zeeman energies at low field in plane of the triangle. This is shown in Figs. 14b-14d that illustrate transformation of the Zeeman levels under the influence of the vibronic coupling obtained with the aid of the general Eq. (22).
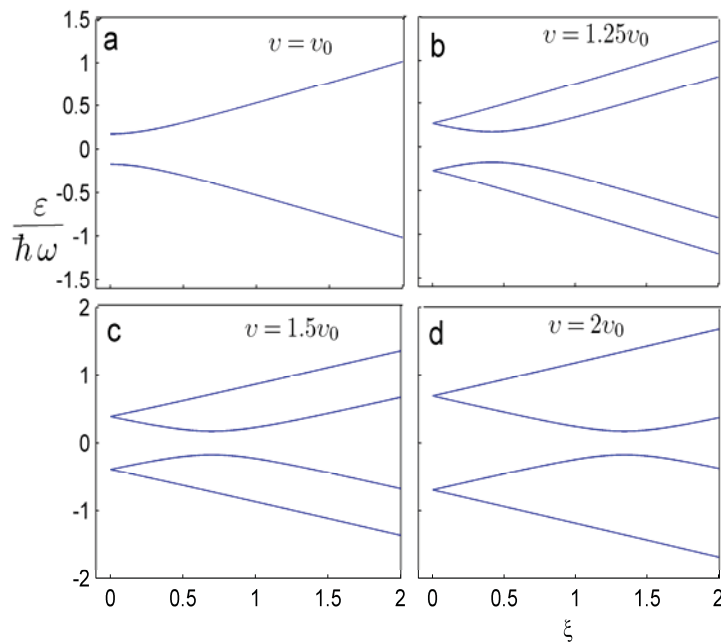
Fig. 14. Influence of the JT interaction (defined by the vibronic coupling parameter υ) on the Zeeman energy pattern in a perpendicular field.
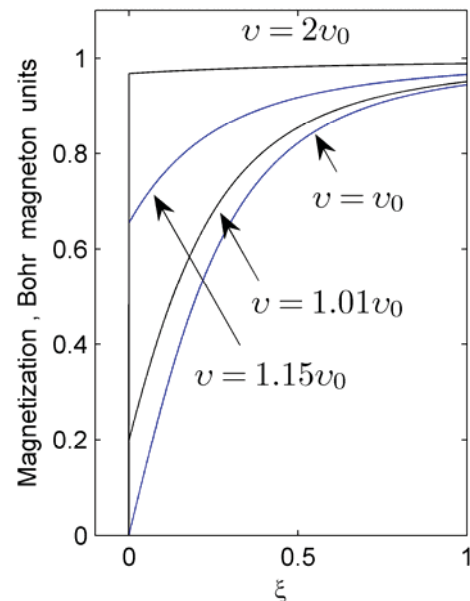
Fig. 15. Influence of the JT interaction on dependence magnetization vs. perpendicular field ($\mathbf{H} \perp C_3$).

Fig. 15 illustrates the influence of the JTE on the field dependence of the magnetization of a triangular unit that is closely related to the influence of the vibronic coupling on the Zeeman pattern (Fig. 14). The magnetization vs. perpendicular field at $T=0$ is presented as a function of the vibronic coupling parameter υ that is assumed to satisfy the condition of instability $\upsilon^2 > \upsilon_0^2 \equiv 4|\delta|/3$. One can see that providing $\upsilon = \upsilon_0$ (and of course $\upsilon < \upsilon_0$ that corresponds to a symmetric stable configuration) the magnetization slowly increases with the increase of the field (due to reduction of the Zeeman interaction in the low field) then reaches saturation when the magnetic field is strong enough to break the AS exchange. Increase of the JT coupling leads to the fast increase of the magnetic moments in the region of low field and formation of the step in magnetization caused by the reduction of the magnetic anisotropy (appearance of the linear terms in the Zeeman levels). This observation is in line of the general concept of the reduction factors in the JT systems. On can see that the semiclassical approach is able to describe this effect. The height of the step depends on the interrelation between AS exchange and vibronic coupling and can be expressed as:

$$M\left(H=0\right)=\frac{g\beta}{2}\frac{E_{JT}}{\sqrt{E_{JT}^2+\delta^2}} \tag{28}$$

The height of the step increases with the increase of the vibronic coupling. Finally, when the JT coupling is strong enough ($\upsilon=2\upsilon_0$) one can observe staircase like behavior of magnetization with the sharp step in which *M(H)* jumps from zero to *M(H* = 0) = gβ/2 at zero field (and T=0) that is expected for a magnetically isotropic system. The influence of the distortions caused by JT instability is very pronounced so that the step starts to appear even when $\upsilon=1.01\,\upsilon_0$. Although the semiclassical description in this range of parameters loses its accuracy the qualitative results are able to draw an adequate physical picture. More accurate quantitative results in this area of vibronic coupling can be obtained by solving the dynamic pseudo JT problem. Another case of interest, strong magnetic field, is discussed in [47]. Numerical estimations [51] show that the vibronic JT parameters for V$_{15}$ are small but the JT coupling is expected to be significant for cooper(II) clusters. In fact, recently very large AS exchange was evoked in [54] in the study of unusual properties of tri- copper clusters. Very strong antiferromagnetic exchange interaction $\left(J=-650cm^{-1}\right)$ has been recently found [55] in a chloride-centered hexanuclear copper(II) cluster that can be a good candidate to test AS exchange in the excited states that exhibit degeneracy (E_1 and E_2 terms) and are expected to be JT active with the significant coupling constants.

SUMMARY

We have given a comprehensive analysis of the unique V_{15} molecular magnetic cluster within the three spin model assuming that the isotropic and AS exchange are acting in the equilateral spin-frustrated trimer. The energy levels behavior and crossover as well as the low-temperature magnetization were studied for different field directions and theoretically explained using pseudo angular momentum representations for the many-spin states. We have indicated the differences between the normal and in-plane parts of the AS exchange interaction and revealed the particular role played by the first at low fields and by the second one in the vicinity of intersection points. Afterwards using pseudo angular quantum numbers we have formulated the selection rules for the EPR transitions and have given comprehensive analysis of the EPR spectra at different frequencies. At the same time we have recognized the high-frequency temperature dependence of the spectral bandwidth as problem which can not be explained within the foregoing model and thus addressing us for studying additional phenomena like relaxation processes and hyperfine structure in vanadium clusters. We succeeded in fitting the results of our calculations to the experimental data for low-temperature magnetization and in this way for the first time precisely estimated the components of AS exchange vectors for the V_{15} molecule. JT instability is shown to eliminate spin frustration due to removal of the "accidental" degeneracy in course of the dynamical structural distortions. The influence of the vibronic interaction on the magnetization is revealed with the aid of the semiclassical adiabatic approach that provides qualitatively transparent results and gives numerical results with a good accuracy. The first and second van Vleck coefficients in the Zeeman energies are deduced as the functions of the direction of the field, AS exchange and vibronic coupling. The JT coupling is shown to be competitive to the AS exchange so that the increase of the vibronic coupling decrease the magnetic anisotropy of the system. On the other hand AS exchange tends to suppress to JTE. This is demonstrated by the theoretical modeling of the field dependence of the magnetization that clearly exhibits crucial role of the pseudo JT coupling in spin-frustrated systems. Furthermore we can conclude that we understand more about the physical contents of the concept of spin frustration and about frustrated systems integrated in complex systems. Therefore, we intend to extend this to other complex systems, e.g. where frustrated systems are interacting like double triangular cluster in $\{Mo_{57}\}\{V_3\}_2$ (see ref [56]). Structure-related magnetism of polyoxometalates from the standpoint of spin frustration in high-nuclearity metal clusters is highlighted in the review article [57].

REFERENCES

[1] A. Müller, J. Döring, Angew. Chem. Int. Ed. Engl. 27 (1988) 1721.

[2] D. Gatteschi, L. Pardi, A.-L. Barra, A. Müller, J. Döring, Nature 354 (1991) 465.

[3] A.-L. Barra, D. Gatteschi, L. Pardi, A. Müller, J. Döring, J. Am. Chem. Soc. 114 (1992) 8509.

[4] D. Gatteschi, L. Pardi, A.-L. Barra, A. Müller, Mol. Eng. 3(1993) 157.

[5] B. Barbara, J. Mol. Struct. 656 (2003) 135.

[6] I. Chiorescu, W. Wernsdorfer, A. Müller, H. Bögge, B. Barbara, Phys. Rev. Lett. 84 (2000) 3454.

[7] I. Chiorescu, W. Wernsdorfer, A. Müller, S. Miyashita, B. Barbara, Phys. Rev.B67 (2003) 020402(R).

[8] S. Miyashita, J. Phys. Soc. Japan, 65 (1996) 2734.

[9] H. Nojiria, T. Taniguchia, Y. Ajiro, A. Müller, B. Barbara, Physica B 346–347 (2004) 216.

[10] S. Miyashita, J. Phys. Soc. Japan, 64 (1995) 3207.

[11] V.V. Platonov, O.M. Tatsenko, V.I. Pils, A.K. Zvezdin, B. Barbara, Physics of the Solid State (Rus. Fizika Tverdogo Tela), 44 (2002) 2010.

[12] J. Kortus, M.R. Pederson, C.S. Hellberg, S.N. Khanna, Eur. Phys. J. D16 (2001) 177.

[13] J. Kortus, C.S. Hellberg, M.R. Pederson, Phys. Rev. Lett. 86 (2001) 3400.

[14] D.W. Boukhvalov, V.V. Dobrovitski, M.I. Katsnelson, A.I. Lichtenstein, B.N. Harmon, P. Kögerler, Phys. Rev. B70 (2004) 054417.

[15] H. De Raedt, S. Miyashita, K. Michielsen, Phys. Stat. Sol. (b) 241 (2004) 1180.

[16] S. Miyashita, H. De Raedt, K. Michielsen, Prog. Theor. Phys. 110 (2003) 889.

[17] H. De Raedt, S. Miyashita, K. Michielsen, M. Machida, Phys. Rev. B70 (2004) 064401.

[18] N.P. Konstantinidis, D. Coffey, Phys. Rev. B 66 (2002) 174426.

[19] G. Chaboussant, R. Basler, A. Sieber, S.T. Ochsenbein, A. Desmedt, R.E. Lechner, M.T.F. Telling, P. Kögerler, A. Müller, H.-U. Güdel, Europhys. Lett. 59 (2) (2002) 291.

[20] G. Chaboussant, S.T. Ochsenbein, A. Sieber, H.-U. Güdel, H. Mutka, A. Müller, B. Barbara, Europhys. Lett. 66 (3) (2004) 423.

[21] I.E. Dzyaloshinsky, Zh.Exp.Teor.Fiz. 32(1957)1547.

[22] T. Moria, Phys. Rev. 120 (1960) 91.

[23] B.S. Tsukerblat, M.I. Belinskii, V.E. Fainzilberg, Magnetochemistry and spectroscopy of transition metal exchange clusters, in: Soviet Sci. Rev. B, Harwood Acad. Pub. (1987), ed. M. Vol'pin, pp. 337– 482.

[24] M.I. Belinskii, B.S. Tsukerblat, A.V. Ablov, Phys. Stat. Solidi (1972) K71.

[25] M.I. Belinskii, B.S. Tsukerblat, Fizika. Tverdogo Tela (Rus), 15 (1973) 29.

[26] B.S. Tsukerblat, M.I. Belinskii, A.V. Ablov, Fizika. Tverdogo Tela (Rus), 16 (1974) 989.

[27] B.S. Tsukerblat, M.I. Belinskii, Magnetochemistry and Radiospectroscopy of Exchange Clusters, Pub. Stiintsa (Rus) Kishinev (1983).

[28] B.S. Tsukerblat, B. Ya. Kuavskaya, M. I. Belinskii, A. V. Ablov, V. M. Novotortsev, V.T. Kalinnikov, Theoretica Chimica Acta 38 (1975) 131.

[29] M.I. Belinskii, B.S. Tsukerblat, A.V. Ablov, Molecular Physics,28 (1974) 283.

[30] B.S. Tsukerblat, V.E. Fainzilberg, M.I. Belinskii, B. Ya. Kuyavskaya, Chem. Phys. Lett. 98 (1983) 149.

[31] B.S. Tsukerblat, B. Ya. Kuyavskaya, V.E. Fainzilberg, M.I. Belinskii, Chem. Phys. 90 (1984) 361; 90 (1984) 373.

[32] V. E. Fainzilberg, M.I. Belinskii, B. Ya. Kuyavskaya, B. S. Tsukerblat, Mol. Phys.,54 (1985) 799.

[33] B.S. Tsukerblat, I.G. Botsan, M.I. Belinskii, V.E. Faiinzilberg, Molec. Phys. 54 (1985) 813.

[34] V.E. Fainzilberg, M.I. Belinskii, B.S. Tsukerblat, Solid State Com. 36 (1980) 639.

[35] V.E. Fainzilberg, M.I. Belinskii, B.S. Tsukerblat, Mol. Phys., 44 (1981) 1177; 44 (1981) 1195; 45 (1982) 807.

[36] Tsukerblat, A. Tarantul, A. Müller, Phys. Lett. A 353 (2006) 48. 35

[37] J. J. Borras-Almenar, J.M.Clemente-Juan, E. Coronado, B.S. Tsukerblat, Inorganic Chemistry, 38 (1999) 6081; J. Comp. Chemistry, 22(2001)985.

[38] B.S. Tsukerblat, Group Theory in Chemistry and Spectroscopy, Academic Press, London,1994; Dover Pub. Inc, Mineola, New York, 2006.

[39] B. Tsukerblat, A. Tarantul, A. Müller , J. Chem. Phys., 125 (2006) 0547141.

[40] T. Sakon, K. Koyama, M. Motokawa, Y. Ajiro, A. Müller, B. Barbara, Physica B 346–347 (2004) 206.

[41] I. Chiorescu , W. Wernsdorfer, A. Müller, H. Bögge, B.Barbara, J.Magn. Magn. Mater., 221 (2000) 103.

[42] M. Machida, T. Iitaka, S. Miyashita, arXiv:cond-mat/0501439 v2 16 Jun 2005.

[43] A. Tarantul, B. Tsukerblat, A. Müller, *Chem. Phys. Let.*, 428 (2006) 36.

[44] A. Tarantul, B. Tsukerblat, A. Müller, *Inorg. Chem.,* 46 (2007) 161.

[45] R. Englman, *The Jahn–Teller Effect in Molecules and Crystals*, Wiley, London, 1972.

[46] I.B. Bersuker and V.Z. Polinger, *Vibronic Interactions in Molecules and Crystals*, Springer-Verlag , Berlin, 1989.

[47] I.B. Bersuker, *The Jahn-Teller Effect*, Cambridge University Press, 2006.

[48] J.J. Borrás-Almenar, E. Coronado, H.M. Kishinevsky, B.S. Tsukerblat, *Chem.Phys.Lett.* 217 (1994) 525.

[49] C.A. Bates and R.F. Jasper, *J.Phys.C: Sol. State Phys*., 4 (1971) 2341.

[50] A. Varshalovich, A. N. Moskalev and V. K. Khersonskii, *Quantum Theory of Angular Momentum*, World Scientific, Singapore, 1988.

[51] B. Tsukerblat**,** A. Tarantul, A. Müller, *J. Mol. Structure*, doi:10.1016/j.molstruc.2006.12.062.

[52] A.I. Popov, V.I. Plis, A. F. Popkov, A.K. Zvezdin, *Phys. Rev.B,* 69 (2004) 104418.

[53] O.Kahn, *Molecular magnetism*, VCH, NY, 1993.

[54] J. Yoon, L. M. Mirica, T. D. P. Stack, E.I. Solomon, *J.Am.Chem.Soc*., 126 (2004) 12586.

[55] A.A. Mohamed, A. Burini, R., Galassi, D. Paglialunga, J. R. Galán-Mascarós, K.R. Dunbar, J. P. Fackler, Jr. *Inorg. Chem*., 46 (2007) 2348.

[56] D. Gatteschi, R. Sessoli, W. Plass, A. Müller, E. Krickemeyer, J. Meyer, D. Sölter, P. Adler, *Inorg. Chem.***,** *3,* (1996) 1926.

[57] P. Kögerler, B. Tsukerblat, A. Müller, *Dalton Transactions* (to be published).